NANO LETTERS

2006
Vol. 6, No. 1
84−88

Multicolor FRET Silica Nanoparticles by Single Wavelength Excitation

Lin Wang and Weihong Tan*

Center for Research at Bio/nano Interface, Department of Chemistry and Shands Cancer Center, UF Genetics Institute and McKnight Brain Institute, University of Florida, Gainesville, Florida 32611-7200

Received October 24, 2005; Revised Manuscript Received December 2, 2005

ABSTRACT

Fluorescent nanoparticles with multiple emission signatures by a single wavelength excitation are needed in multiplex bioanalysis and molecular imaging. We have prepared silica nanoparticles encapsulated with three organic dyes using a modified Stöber synthesis method. By varying the doping ratio of the three tandem dyes, fluorescence resonance energy transfer (FRET)-mediated emission signatures can be tuned to have the nanoparticles exhibit multiple colors under one single wavelength excitation. These nanoparticles are intensely fluorescent, highly photostable, uniform in size, and biocompatible. The acceptor emission of the FRET nanoparticles has generated a large Stokes shift, which implicates broad applications in biological labeling and imaging. Molecular recognition moieties, such as biotin, can be covalently attached to the nanoparticle surface to allow for specific binding to target molecules. These multicolor FRET silica nanoparticles can be used as barcoding tags for multiplexed signaling. By using these NPs, one can envision a dynamic, multicolor, colocalization methodology to follow proteins, nucleic acids, molecular machines, and assemblies within living systems.

The need to decipher many biological events simultaneously has driven the development of multiplexed fluorescent tags. However, the number of available dyes that have single wavelength excitation and distinguishable emission maxima is limited. In addition, the fluorescent signal from dye molecules is weak, and the dye molecules are susceptible to irreversible photodestruction. To address these issues, barcoding nanoparticles (NPs) have been developed to serve as alternative substrates for multiplexed bioassays.[1−8] Barcoding NPs have exhibited advantages over energy transfer fluorescent dyes[9] in that the NPs are not vulnerable to photobleaching or degradation in the complex environment, their optical signal is higher than single dye molecules, and a large barcoding library can be built. Quantum dots (QDs) have attracted great interest in this area because of their broad excitation spectra and tunable emission wavelengths.[1−2] In a proof-of-concept investigation, it is estimated that by using QDs with just 6 colors in 10 different intensities, a library of approximately one million entries could be encoded.[1] However, QDs are relatively difficult to be prepared reproducibly, and the surface modification chemistry is still under investigation. In addition, the "blinking" characteristic is a limiting factor for raster scanning systems such as confocal microscopy and flow cytometry. QD's cytotoxicity is of concern for in vivo applications.[10] Commercially available fluorescent polymer or latex NPs and microspheres have been utilized in various biological applications. For instance, arrays of fluorescent polymer microspheres that differ in intensity, size, or excited-state lifetime have been used extensively in simultaneous assays to determine multiple analytes in a single sample. TransFluoSpheres beads (Molecular Probes) incorporate two or more fluorescent dyes that undergo excited-state energy transfer, exhibit large Stokes shifts, and match different excitation sources. These beads can be used in the major microsphere-based diagnostic test systems and in experiments that measure regional blood flow, study phagocytosis, detect cell-surface antigens, and trace neurons.[11] Recently, we have reported using nonblinking, bright, and photostable silica NPs and dual-luminophore-doped silica NPs for multiplexed signaling.[7] Compared to polymer NPs, silica NPs possess several advantages: (i) Silica NPs are easy to separate via centrifugation during particle preparation, surface modification, and other solution treatment processes because of the high density of silica (e.g., 1.96 g/cm^3 for silica vs 1.05 g/cm^3 for polystyrene); (ii) Silica NPs are hydrophilic and biocompatible, not subject to microbial attack. There is no swelling or porosity change with pH changes,[12] while polymer particles are hydrophobic, tend to agglomerate in aqueous medium, and swell in organic solvents, resulting in dye leakage. In the dual-luminophore-doped silica NP barcoding system, two types of inorganic luminophores, RuBpy and OsBpy, were encapsulated into silica NPs using the reverse micelle or water-in-oil (W/O) microemulsion system. By precisely controlling the doping ratios, we generated multiple unique NP emission signatures

* Corresponding author. Phone and fax: 352-846-2410. E-mail: tan@chem.ufl.edu.

10.1021/nl052105b CCC: $33.50
Published on Web 12/20/2005

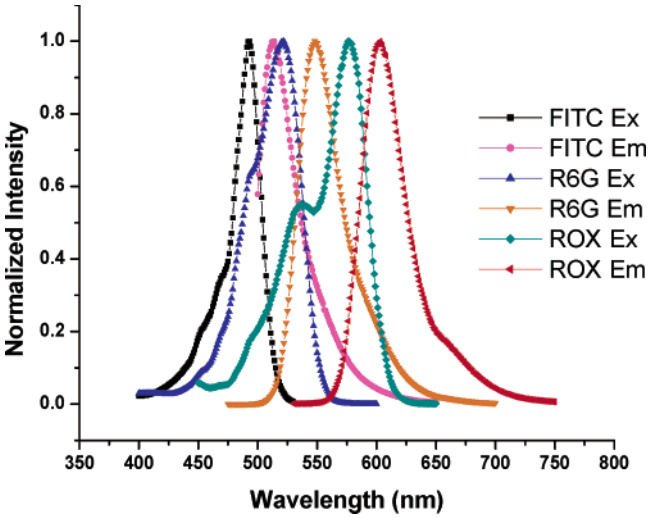

Figure 1. Normalized excitation and emission spectra of FITC, R6G, and ROX dyes in pH 7.4 phosphate buffer.

where a single light source was sufficient for reading all of the NPs. However, inorganic dyes have relatively low quantum yields and the dual-luminophore-doped NPs fall short of abundant color combinations, which limits their use in multicolor imaging applications. To generate versatile colors, a new strategy is to incorporate multiple energy transfer fluorescent dyes into silica NPs.[13] By varying the doping ratio of the three tandem dyes, fluorescence resonance energy transfer (FRET)-mediated emission signatures can be tuned, and the NPs exhibit different colors under one single wavelength excitation. A large number of NP barcodes can be generated from a limited number of individual fluorophores. Another potential advantage of the FRET NPs is the large Stokes shift, which benefits applications in complex biological milieu.

Triple-dye-doped FRET silica NPs were prepared via a modified Stöber synthesis method.[14−15] The three tandem dyes were chosen carefully to allow for efficient fluorescence resonance energy transfer. FITC, R6G, and ROX were employed in our model construction because of their effective spectral overlapping (Figure 1). In the triple-dye-doped NPs, FITC was used as a common donor for R6G and ROX, while R6G acted as both an acceptor for FITC and a donor for ROX. To prepare the NPs, the three types of amine reactive dye molecules were first covalently linked to the silane coupling agent APTS [(3-aminopropyl)triethoxysilane]: FITC-SE [5-(and-6)-carboxyfluorescein, succinimidyl ester], R6G-SE [5-carboxyrhodamine 6G, succinimidyl ester], and ROX-SE [6-carboxy-X-rhodamine, succinimidyl ester] were individually dissolved in 1.5 mL of anhydrous DMF, combined with an excess of APTS at a molar ratio of dye to APTS of 1:2, and stirred under a dry nitrogen atmosphere for 24 h in the dark. Second, the three APTS-dye conjugates were mixed at desired ratios and added to a clean glass reaction vessel containing 16.75 mL of pure ethanol and 1.28 mL of ammonium hydroxide (28.8%). The mixture was stirred for 24 h. TEOS (tetraethyl orthosilicate, 0.71 mL) was added afterward and stirred for another 24 h. After the reaction, the samples were centrifuged at 14 000 rpm for 30 min to collect the silica NPs. The NPs were further washed with ethanol and deionized water by centrifugation and decantation several times to remove the unreacted chemicals.

During our initial preparation process, TEOS was introduced immediately after APTS-dye conjugates were added to the basic ethanol solution. However, we found that there was rather low FRET efficiency between the dyes. As shown in Figure 2a, the peak intensity ratios (measured at 520, 550, and 605 nm, respectively) of the triple-dye-doped NPs (dye doping ratio = 1:1:1) are 1:0.8:0.4. ROX dye exhibits a weak fluorescence signal because of the low FRET efficiency. It is known that FRET is mediated by a dipole−dipole coupling between chromophores and the FRET efficiency is proportional to the inverse sixth power of the distance between the chromophores.[16] The FRET efficiency between an α-naphthyl energy donor group and a dansyl energy acceptor group has been found to be 100% at a distance of 1.2 nm and 16% at 4.6 nm.[17] The low FRET efficiency implies a large separation distance between the dyes encapsulated inside the NPs. Our reasoning is based on the following: (i) the APTS-dye conjugates must be hydrolyzed to be incorporated into the silica matrix, it is likely that the hydrolysis reaction rates of each APTS-dye conjugates are different, so the three dyes are encapsulated into different silica layers, and the spacer shells in between reduce the FRET efficiency; (ii) the

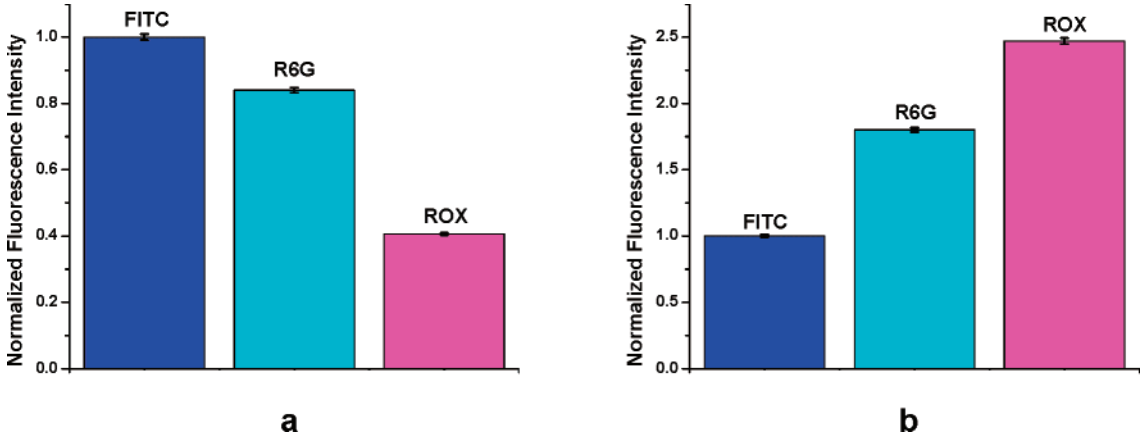

Figure 2. Normalized three peak intensity ratios of FRET NPs (dye doping ratio = 1:1:1) without (a) and with (b) prehydrolyzing the APTS−dye conjugates for 24 h.

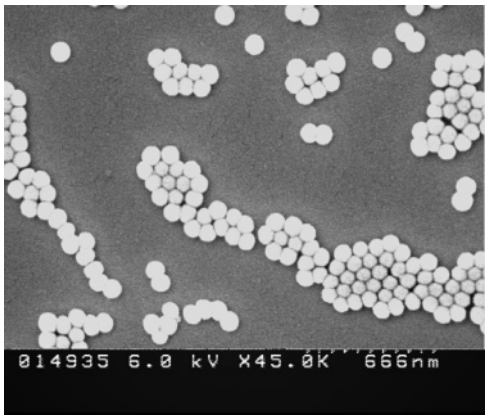

Figure 3. SEM image of triple-dye-doped NPs. The NPs are in the range of 70 nm. The NP size can be controlled with different parameters in synthesis.

hydrolysis rate of APTS is five times slower than that of TEOS because of the electron-donating capacity of the alkyl group, and siloxane bond formation is much faster than the hydrolysis step;[18] therefore, TEOS could be converted entirely to silica NPs before a large number of dyes are housed inside. The FRET efficiency is low because of a large portion of the dyes not being incorporated into the particles during synthesis or because of physical separation of the FRET pairs. To address these challenges, the three APTS−dye conjugates were mixed and prehydrolyzed for 24 h before beginning the colloid formation by the addition of TEOS. This strategy not only ensures a greater amount and equal opportunity of the dyes incorporated during NP synthesis but also allows the formation of small dimers or oligomers between the APTS−dye conjugates. The possible formation of such dye clusters made fluorophores covalently attached to one another and shortened the distance between them to the benefit of the FRET efficiency (Figure 2b). However, it should be mentioned that the close proximity of the fluorophores might also lead to self-quenching between identical species, so the dye-loading amount was experimentally optimized to find a compromise between minimal self-quenching and maximal FRET efficiency.

Single dye-(ROX) and triple-dye-(FITC:R6G:ROX = 1:1:1) doped silica NPs were prepared following the aforementioned procedures and characterized with respect to their size, morphology, photostability, and optical/spectral properties. The resultant NPs exhibit several remarkable features that show the clear advantages of these NPs. (i) The NPs were fairly uniform in size ($\Phi = 70 \pm 5$ nm) as shown in the SEM image (Figure 3). The NP size can be controlled by changing the amounts of ammonium hydroxide while other parameters remain constant. For example, the NP size was decreased to 25 nm by reducing the amount of ammonium hydroxide to 412 μL (1/3 of the initial value). (ii) A large number of dye molecules were housed inside one NP that exhibits an extraordinary fluorescent signal. To estimate the amount of dye molecules encapsulated inside one NP, we employed single-dye-doped ROX NPs because of the difficulty of characterizing triple-dye-doped NPs where the fluorescence intensity corresponding to FITC and R6G was suppressed by energy transfer. The titration curve of the fluorescence intensity as a function of the ROX dye concentration was obtained first. The NP concentration was then determined by drying and weighing a certain volume of NP solution. The fluorescence intensity of 10^{-11} M ROX NP was measured, and the effective fluorescence intensity of a single NP ($\Phi = 70$ nm) was calculated to be around 2000 times that of a single fluorophore. This high signal amplification is essential to addressing the growing need for highly sensitive bioassays. (iii) The NPs were colloidally stable, and no dye leakage was observed from the NPs. The ROX NPs dissolved in 10 mM phosphate buffer (pH = 7.4) remained physically stable over one month without any aggregation or settling. The NP solution was centrifuged, and the fluorescence intensity of the supernatant was monitored on different days. A negligible amount of fluorescence was obtained in the supernatant compared to the NPs. No obvious dye leakage was observed because the dyes were covalently linked to the silica matrix. (iv) The silica matrix provides the NPs with a high photobleaching threshold that makes them highly appealing for labeling in both long-term in vivo cellular imaging and in vitro assay detections. In our experiment, a 10^{-14} M ROX NP solution was exposed to continuous intensive excitation with a 150-watt xenon lamp and the fluorescence intensity was monitored. The fluorescence intensity remained constant, and no obvious photobleaching was observed for a period of 1 h, while under the same experimental conditions, the pure ROX dye solution lost more than 80% of the original signal. In another demonstration, we tested the photostability of the NPs with CEM cancer cells. The CEM cancer cells were bound with aptamer conjugated dye-doped NPs via receptor−aptamer recognition, and the images were taken on a confocal microscope. After intense laser excitation for 30 min, no noticeable fluorescence degradation was observed. (v) Post-coating can be applied easily to introduce suitable functional groups for further attaching biological moieties on the NPs. To functionalize the NPs with amine groups, approximately 10 mg of NPs were dispersed in 1 mL of deionized water followed by the addition of 20 μL of glacial acetic acid. (3-Trimethoxysilylpropyl) diethylenetriamine (20 μL) was then added, and the suspension was stirred for 3−4 h at room temperature. The particles were washed three times with 10 mM MES buffer (pH = 5.5) and dispersed in the same buffer. Similar post-coating procedures can be employed to modify the NP surface with carboxyl or thiol groups, phosphorate groups, and so forth. After the NPs are modified with different functional groups, they can act as a scaffold for the grafting of biological moieties by means of standard bioconjugation schemes. (vi) The relative peak intensity ratios of the triple-dye-doped NPs exhibit good batch-to-batch reproducibility. For instance, the peak intensity ratios from five parallel NP solutions (dye doping ratio = 1:1:1) were compared and the coefficient of variation was 0.9%. This small coefficient of variation clearly shows the reproducibility in our current synthesis of these NPs.

To test whether multiple fluorophores could be coencapsulated into NPs and that FRET did take place, we prepared

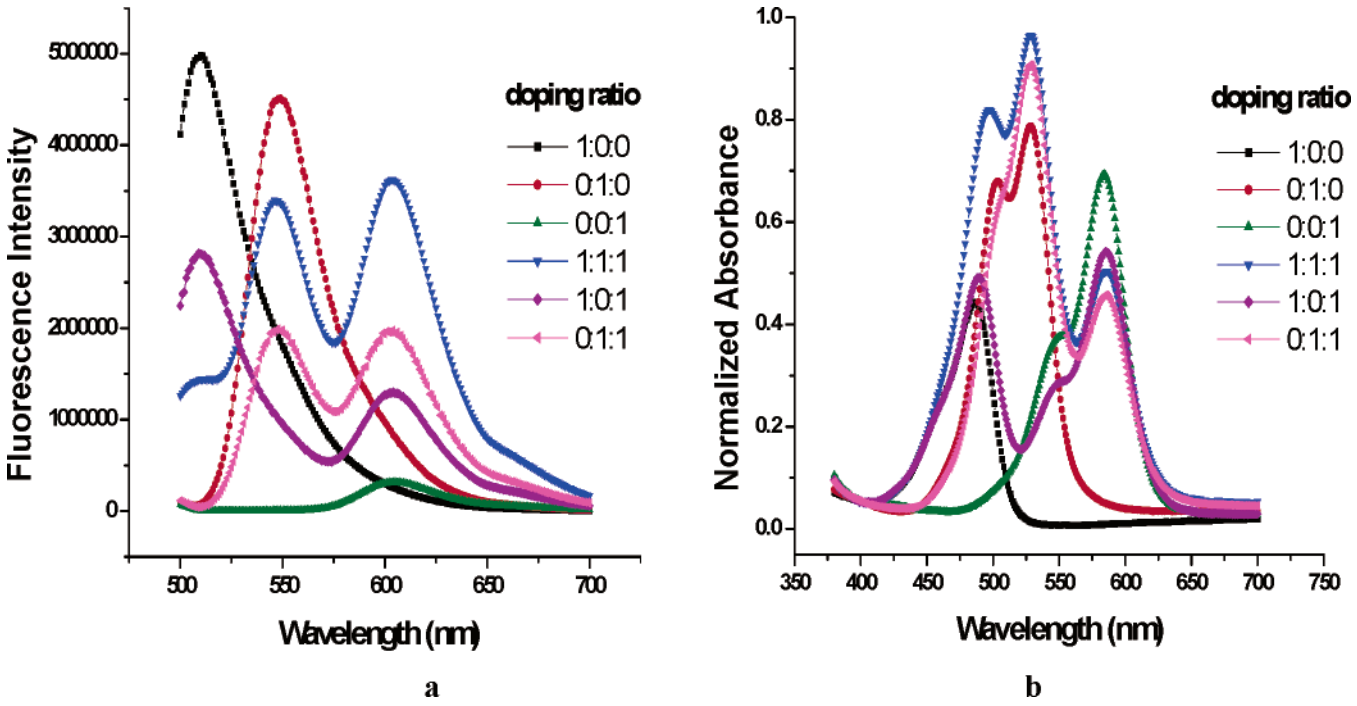

Figure 4. (a) Fluorescence emission spectra of NP samples encapsulated with one, two, or three types of fluorophores and (b) the corresponding normalized absorption spectra.

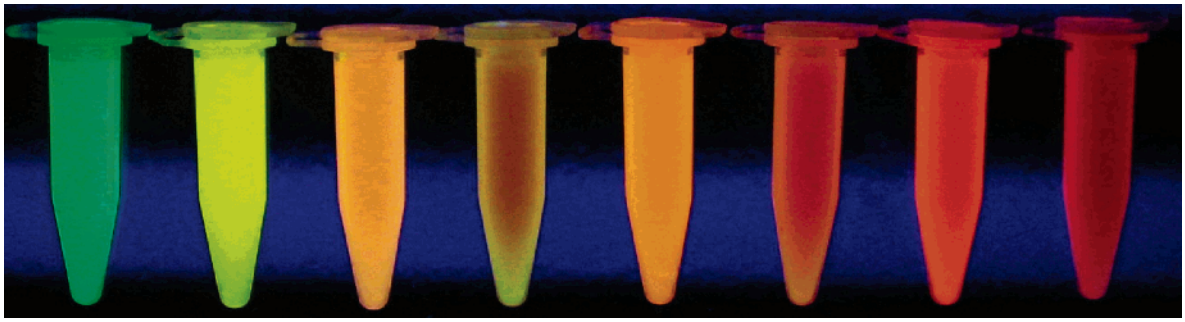

Figure 5. NP samples with different doping dye combinations under 300-nm UV illumination. Dye doping ratio (in order): 1:0:0, 0:1:0, 1:0:1, 4:1.5:3, 0.5:0.5:0.5, 2:2:2, 0:1:1, 0.5:0.5:4.

six FRET NP tags, each containing one, two, or three types of fluorophores. Figure 4a shows the nonnormalized fluorescence spectra of the same concentration of the NPs by exciting at a single wavelength of 488 nm. Comparing the emission spectrum of triple-dye-doped (dye doping ratio = 1:1:1) NPs with that of single- or dual-dye-doped NPs, the decreased emission of FITC and dramatically increased emission of ROX demonstrates efficient FRET between dyes in a particle. The corresponding absorption spectra (Figure 4b) of the six dye-doped NP solutions were normalized by subtracting the absorbance of the same concentration of the pure silica NPs. The resultant spectra also prove successful loading of multiple fluorophores inside one NP. Although the concentrations of the three respective dye solutions were equivalent, the absolute absorbance of single-dye-doped NPs varied from one another, which could be attributed to the different extinction coefficients of the three dyes (ϵ_{FITC}: 68 000, ϵ_{R6G}: 116 000, ϵ_{ROX}: 82 000 M^{-1} cm^{-1}).

By varying the relative concentrations of each dye, the FRET-mediated NP emission signatures can be adjusted and the NPs exhibit different colors under UV illumination (Figure 5) or laser excitation on a confocal microscope (Figure 6b). To demonstrate the biobarcoding capabilities of multicolor FRET silica NPs, we employed a simplified avidin−biotin binding assay. Amine-modified NPs doped with three dyes at various ratios were reacted with the activated ester of biotin (NHS-PEG_{5000}-biotin) to couple biotin molecules to the NPs. PEG linkers functioned to orient the biotin molecules far away from the NP surface to ensure the flexibility of binding to a target. Streptavidin-coated microspheres and biotin-labeled NPs were then mixed at a 1:50 000 ratio to ensure sufficient saturation of the microsphere surface,[7a] and the mixture was shaken slowly for 2 h at room temperature. The complexes were centrifuged and washed several times with phosphate buffer to remove the unbound NPs. The SEM and confocal images of the resultant microsphere−NP complexes display that streptavidin-coated microspheres were densely covered with biotin-labeled NPs (Figure 6a) and exhibited the coding colors of the attached NPs. Five microsphere-NP complexes were mixed together and excited with a 488-nm Argon-ion laser, and the five distinguishable colors were clearly observed simultaneously

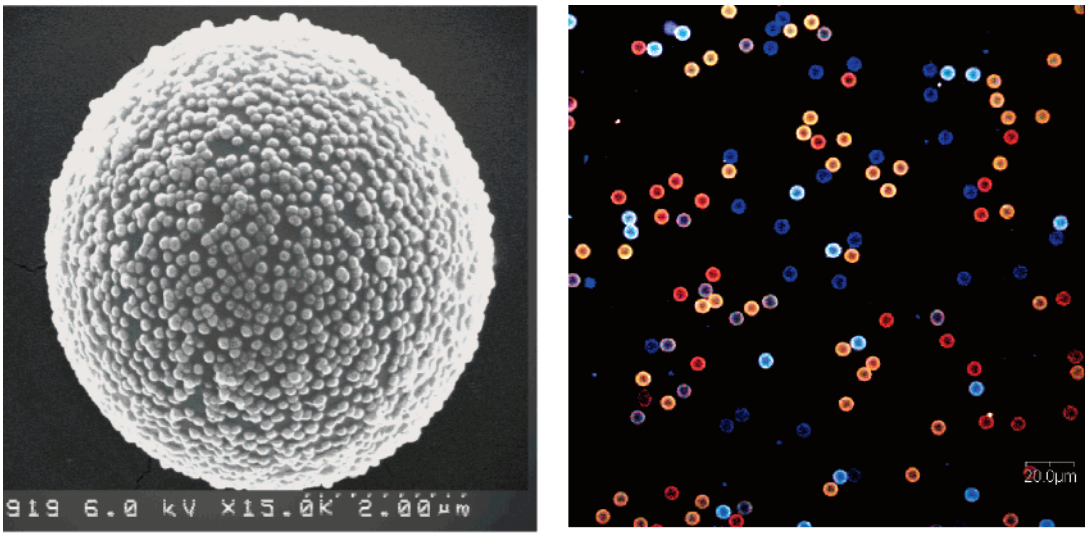

a b

Figure 6. (a) SEM image of one microsphere−NP complex (b) Confocal fluorescence image of a mixture of five types of microsphere−NP complexes under 488-nm Argon-ion laser excitation.

(Figure 6b). This model demonstrated the potential of using multicolor FRET NPs for multiplexed bioassays. The barcoding NPs can be conjugated with aptamers or antibodies for specific recognition of the receptors/antigens on the surface of a cell or bacterium. Currently, intensive research using multicolor NPs for imaging multiple bacterial species simultaneously is being conducted in our lab.

In summary, FRET has been reported as a tool to construct barcoding silica NPs for multiplexed signaling. By varying the ratio of the three tandem dyes coencapsulated into the silica NPs, the NPs exhibit multicolors under one single wavelength excitation. The NPs can be made with different sizes via easy control of synthetic parameters. They are uniform, exhibit high fluorescence intensity and excellent photostability, and can be labeled easily with biomolecules such as proteins and nucleic acids. One other potential advantage of FRET NPs is that by optimizing the amount of dye molecules in a NP, the emission spectrum can be tuned so that only the longest-wavelength dye will exhibit significant fluorescence at a short-wavelength excitation. This feature will overcome the challenge of the small Stokes shift of many organic dyes, enabling the NPs to be detected in samples with significant Rayleigh/Raman scattering or with endogenous fluorescent compounds. It is also noteworthy that the covalent trichromophoric labeling approach can be further extended to more than three chromophores; the FRET NP strategy can be applied to any energy transfer dye series. The significance of this study lies in that it provides highly fluorescent and photostable barcoding NPs that permit simultaneous and sensitive detection of multiple targets as well as opens up a new perspective in the design of multifunctional structures based on silica NPs, which have seen a variety of interesting applications in the past few years.[19−20]

Acknowledgment. We thank Dr. Charles Lofton for interesting discussions about this work. This work was supported by NSF NIRT and NIH grants.

References

(1) Han, M.; Gao, X.; Su, J. Z.; Nie, S. *Nat. Biotechnol*. **2001**, *19*, 631.
(2) Jaiswal, J. K.; Mattousi, H.; Mauro, J. M.; Simon, S. M. *Nat. Biotechnol.* **2003**, *21*, 47.
(3) Schultz, S.; Smith, D. R.; Mock, J. J.; Schultz, D. A. *Proc. Natl. Acad. Sci. U.S.A.* **2000**, *97*, 996.
(4) Nam, J.; Park, S.; Mirkin C. A. *J. Am. Chem. Soc.* **2002**, *124*, 3820.
(5) Walton, I. D.; Norton, S. M.; Balasingham, A.; He, L.; Oviso, D. F.; Gupta, D.; Raju, P. A.; Michael, M. J.; Freeman, R. G. *Anal. Chem.* **2002**, *74*, 2240.
(6) Lawrie, G. A.; Battersby, B. J.; Trau, M. *Adv. Funct. Mater.* **2003**, *13*, 887.
(7) (a) Wang, L.; Yang, C.; Tan, W. *Nano Lett.* **2005**, *5*, 37. (b) Tan, W.; Wang, K.; He, X.; Zhao, X.; Drake, T.; Wang, L.; Bagwe, R. *Med. Res. Rev.* **200**4, *24*, 621.
(8) Kürner, J. M.; Klimant, I.; Krause, C.; Pringsheim, E.; Wolfbeis, O. S. *Anal. Biochem.* **2001**, *297*, 32.
(9) Tong, A. K.; Li, Z.; Jones, G. S.; Russo, J. J.; Ju, J. *Nat. Biotechnol*. **2001**, *19*, 756.
(10) (a) Medintz, I. L.; Uyeda, H. T.; Goldman, E. R.; Mattoussi, H. *Nat. Mater.* **2005**, *4*, 435. (b) Michalet, X.; Pinaud, F. F.; Bentolila, L. A.; Tsay, J. M.; Doose, S.; Li, J. J.; Sundaresan, G.; Wu, A. M.; Gambhir, S. S.; Weiss, S. *Science* **2005**, *307*, 538.
(11) Haugland, R. P. *Handbook of Fluorescent Probes*, 10th ed., 208; http://probes.invitrogen.com/handbook.
(12) Jain, T. K.; Roy, I.; De, T. K.; Maitra, A. *J. Am. Chem. Soc.* **1998**, *120*, 11092.
(13) Montalti, M.; Prodi, L.; Zaccheroni, N.; Zattoni, A.; Reschiglian, P.; Falini, G. *Langmuir* **2004**, *20*, 2989.
(14) Stöber, W.; Fink, A.; Bohn, E. *J. Colloid Interface Sci.* **1968**, *26*, 62.
(15) (a) van Blaaderen, A.; Vrij, A. *Langmuir* **1992**, *8*, 2921. (b) Veraegh, N.; van Blaaderen, A. *Langmuir* **1994**, *10*, 1427.
(16) Förster, Th. In *Modern Quantum Chemistry; Istanbul Lectures*, Part III; Sinanoglu, O., Ed.; Academic: New York, 1965; p 93.
(17) Stryer, L.; Haugland, R. P. *Proc. Natl. Acad. Sci. U.S.A.* **1967**, *58*, 719.
(18) van Blaaderen, A.; Vrij, A. *J. Colloid Interface Sci.* **1993**, *156*, 1.
(19) (a) Zhao, X.; Dytocio, T. R.; Tan, W. *J. Am. Chem. Soc*. **2003**, 125, 11474. (b) Zhao, X.; Bagwe, R.; Tan, W. *Adv. Mater.* **2004**, *16*, 173.
(20) (a) Zhao, X.; Hilliard, L.; Mechery, S.; Wang, Y.; Bagwe, R.; Jin, S.; Tan, W. *Proc. Natl. Acad. Sci. U.S.A.* **2004**, *101*, 15027. (b) Santra, S.; Zhang, P.; Wang, K.; Tapec, R.; Tan, W. *Anal. Chem.* **2001**, *73*, 4988.

NL052105B